

CHARACTERIZATION OF NON-WSSUS FADING DISPERSIVE CHANNELS

Gerald Matz

Institute of Communications and Radio-Frequency Engineering, Vienna University of Technology
Gusshausstrasse 25/389, A-1040 Wien, Austria
phone: +43 1 58801 38916, fax: +43 1 58801 38999, email: g.matz@ieee.org
web: <http://www.nt.tuwien.ac.at/dspgroup/gmatz.html>

ABSTRACT

We present several novel tools for the statistical characterization of fading dispersive channels that do not satisfy the usual WSSUS assumption. A *local scattering function*, describing the time- and frequency-dependent average scatterer power, is introduced. Furthermore, a novel *channel correlation function* is presented that quantifies the scatterer correlation. Based on the channel correlation function, we introduce the practically important class of *doubly underspread channels*. Numerical results involving a simulated and a measured channel illustrate the usefulness of our framework.

1. INTRODUCTION

Realistic models for fading dispersive channels are vital for the design, simulation, and performance evaluation of wireless systems. For linear, time-varying (LTV) random channels, usually the assumption of *wide-sense stationary uncorrelated scatterers* (WSSUS) [1–5] is invoked. Unfortunately, practical wireless channels never satisfy the WSSUS assumption *exactly*. Thus, in this paper we establish a novel framework for the characterization of non-WSSUS channels. The main results can be summarized as follows:

- We introduce the *local scattering function* as an extension of the ordinary scattering function to the non-WSSUS case, and we show that it can be interpreted as a time-frequency (TF) dependent average scatterer power.
- We define a new *channel correlation function* that extends the TF correlation function of WSSUS channels. The channel correlation function is used to define a stationarity time T_s and a stationarity bandwidth F_s within which the channel can be approximated by a WSSUS channel.
- Based on the channel correlation function, we introduce the concept of *doubly underspread channels* that are characterized by a small delay-Doppler spread and slow TF variation of the local scattering function. We demonstrate that practical channels are indeed doubly underspread.

Related Work. Doubly underspread channels are similar in spirit to quasi-WSSUS channels, introduced in a less rigorous way in [2]. Methods for quantifying channel nonstationarities have been described in [6, 7]. Finally, channel models incorporating large-scale fluctuations (path loss, delay drift, shadowing, etc.) have been presented in [8–10].

2. PREREQUISITES

We first briefly review the description of LTV channels and the statistical characterization of WSSUS channels.

Characterization of LTV Channel. The input-output relation of an LTV channel \mathbf{H} is¹

$$r(t) = (\mathbf{H}s)(t) = \int h(t, \tau) s(t - \tau) d\tau.$$

Here, $s(t)$ is the transmit signal, $r(t)$ is the received signal, and $h(t, \tau)$ is the impulse response of \mathbf{H} . Alternative channel descriptions are the *time-varying transfer function* [2, 4, 5, 11], defined as $L_{\mathbf{H}}(t, f) \triangleq \int h(t, \tau) e^{-j2\pi f\tau} d\tau$, and the (*delay-Doppler*) *spreading function* [2, 4, 5], given by $S_{\mathbf{H}}(\tau, \nu) \triangleq \int h(t, \tau) e^{-j2\pi\nu t} dt$. The spreading function characterizes the reflectivity of scatterers associated to delay τ and Doppler ν . We note that time-varying transfer function and spreading function are a 2-D Fourier transform pair.

WSSUS Channels. If the channel \mathbf{H} is assumed to be WSSUS,² the 4-D correlation functions of the spreading function and of the transfer function simplify according to [1, 2]

$$E\{S_{\mathbf{H}}(\tau, \nu) S_{\mathbf{H}}^*(\tau', \nu')\} = C_{\mathbf{H}}(\tau, \nu) \delta(\nu - \nu') \delta(\tau - \tau'), \quad (1)$$

$$E\{L_{\mathbf{H}}(t, f) L_{\mathbf{H}}^*(t', f')\} = R_{\mathbf{H}}(t - t', f - f'). \quad (2)$$

Here, $C_{\mathbf{H}}(\tau, \nu)$ and $R_{\mathbf{H}}(\Delta t, \Delta f)$ are the channel's *scattering function* and *TF correlation function* that are related as [1–3]

$$C_{\mathbf{H}}(\tau, \nu) = \iint R_{\mathbf{H}}(\Delta t, \Delta f) e^{-j2\pi(\nu\Delta t - \tau\Delta f)} d\Delta t d\Delta f. \quad (3)$$

Thus, for WSSUS channels the spreading function is 2-D white and the transfer function is 2-D stationary with power spectral density (PSD) given by $C_{\mathbf{H}}(\tau, \nu)$.

The *delay power profile* and the *Doppler power profile* are respectively defined as [1, 3]

$$P_{\mathbf{H}}(\tau) \triangleq \int C_{\mathbf{H}}(\tau, \nu) d\nu, \quad Q_{\mathbf{H}}(\nu) \triangleq \int C_{\mathbf{H}}(\tau, \nu) d\tau.$$

Their Fourier transforms, $p_{\mathbf{H}}(\Delta f) = R_{\mathbf{H}}(0, \Delta f)$ and $q_{\mathbf{H}}(\Delta t) = R_{\mathbf{H}}(\Delta t, 0)$, are known as *time correlation function* and *frequency correlation function*, respectively [1–3]. Finally, $\bar{\rho}_{\mathbf{H}}^2 \triangleq \int P_{\mathbf{H}}(\tau) d\tau = \int Q_{\mathbf{H}}(\nu) d\nu$ is the channel's *path loss*.

3. CHARACTERIZATION OF NON-WSSUS CHANNELS

We next analyze channels that are not WSSUS. In contrast to (1) and (2), this means that i) the spreading function $S_{\mathbf{H}}(\tau, \nu)$

¹All integrals are from $-\infty$ to ∞ .

²Hereafter, without loss of generality, $h(t, \tau)$, $S_{\mathbf{H}}(\tau, \nu)$, and $L_{\mathbf{H}}(t, f)$ are assumed to be zero-mean 2-D random processes.

is no longer white, i.e., scatterers with different delay or Doppler are correlated (these correlations typically correspond to waves reflected by the same physical object) and ii) the TF transfer function $L_{\mathbf{H}}(t, f)$ is a 2-D *nonstationary* process (e.g., due to large-scale fluctuations). These correlations/nonstationarities are described by the (deterministic) 4-D correlation functions

$$R_S(\tau, \nu; \Delta\tau, \Delta\nu) \triangleq \mathbb{E}\{S_{\mathbf{H}}(\tau, \nu + \Delta\nu) S_{\mathbf{H}}^*(\tau - \Delta\tau, \nu)\}, \quad (4a)$$

$$R_L(t, f; \Delta t, \Delta f) \triangleq \mathbb{E}\{L_{\mathbf{H}}(t, f + \Delta f) L_{\mathbf{H}}^*(t - \Delta t, f)\}. \quad (4b)$$

The 4-D correlation functions in (4) have been considered too cumbersome to be of practical use. On the other hand, the scattering function $C_{\mathbf{H}}(\tau, \nu)$ and the TF correlation function $R_{\mathbf{H}}(\Delta t, \Delta f)$ are no longer well-defined. We resolve this problem by introducing two novel second-order channel statistics that have a clear and intuitive physical meaning and can be viewed as proper extensions of the scattering function and the TF correlation function to the non-WSSUS case.

3.1. Local Scattering Function

Definition and Interpretation. For WSSUS channels, the scattering function is the 2-D PSD of the stationary process $L_{\mathbf{H}}(t, f)$. For non-WSSUS channels, $L_{\mathbf{H}}(t, f)$ is nonstationary and thus its PSD, the scattering function, is not defined. However, motivated by time-varying power spectra of nonstationary processes (see e.g. [12]), we define a *local scattering function* as

$$\begin{aligned} \mathcal{C}_{\mathbf{H}}(t, f; \tau, \nu) &\triangleq \iint R_L(t, f; \Delta t, \Delta f) e^{-j2\pi(\nu\Delta t - \tau\Delta f)} d\Delta t d\Delta f \\ &= \iint R_S(\tau, \nu; \Delta\tau, \Delta\nu) e^{-j2\pi(f\Delta\tau - t\Delta\nu)} d\Delta\tau d\Delta\nu. \end{aligned}$$

Note that this definition is consistent with the WSSUS case where one has $\mathcal{C}_{\mathbf{H}}(t, f; \tau, \nu) = C_{\mathbf{H}}(\tau, \nu)$. Unfortunately, in general, $\mathcal{C}_{\mathbf{H}}(t, f; \tau, \nu)$ is not necessarily real-valued and positive (however, it is approximately positive in the case of doubly underspread channels considered in Section 4).

In a certain sense, the local scattering function describes the mean power of scatterers causing a delay/Doppler shift (τ, ν) at time t and frequency f . This interpretation can be supported as follows. Consider a test signal $g(t)$ that is well TF localized about the origin of the TF plane. Transmitting the signal $g_{t_0 - \tau_0, f_0}(t) = g(t - t_0 + \tau_0) e^{j2\pi f_0 t}$ (localized about the TF point $(t_0 - \tau_0, f_0)$) over the channel \mathbf{H} and taking the inner product of the received signal $(\mathbf{H}g_{t_0 - \tau_0, f_0})(t)$ with $g_{t_0, f_0 + \nu_0}(t) = g(t - t_0) e^{j2\pi(f_0 + \nu_0)t}$ (which is localized about $(t_0, f_0 + \nu_0)$) yields a measure of the energy transfer from $(t_0 - \tau_0, f_0)$ to $(t_0, f_0 + \nu_0)$ effected by \mathbf{H} . On average, this TF energy transfer can be shown to equal

$$\mathbb{E}\{|\langle \mathbf{H}g_{t_0 - \tau_0, f_0}, g_{t_0, f_0 + \nu_0} \rangle|^2\} = (\mathcal{C}_{\mathbf{H}} *_d K_g)(t_0, f_0; \tau_0, \nu_0), \quad (5)$$

where $*_d$ denotes d -dimensional convolution and $K_g(t, f; \tau, \nu)$ is a ‘‘smoothing kernel’’ that can be shown to be effectively nonzero only for $(t, f; \tau, \nu)$ close to $(0, 0; 0, 0)$. Hence, (5) implies that a smoothed version of $\mathcal{C}_{\mathbf{H}}(t, f; \tau, \nu)$ is positive and describes the average TF energy transfer from the TF location $(t_0 - \tau_0, f_0)$ to the TF location $(t_0, f_0 + \nu_0)$. A similar conclusion can be drawn from the I/O-relation

$$\overline{W}_r(t, f) = \iint \mathcal{C}_{\mathbf{H}}(t, f - \nu; \tau, \nu) \overline{W}_s(t - \tau, f - \nu) d\tau d\nu, \quad (6)$$

where $\overline{W}_s(t, f)$ and $\overline{W}_r(t, f)$ denote the *Rihaczek spectrum* [12] of the transmit signal $s(t)$ (assumed statistically independent of \mathbf{H}) and the received signal $r(t)$, respectively. For WSSUS channels, (6) reduces to the well-known relation $\overline{W}_r(t, f) = (C_{\mathbf{H}} *_2 \overline{W}_s)(t, f)$.

Induced Channel Statistics. Extending the WSSUS case (cf. Section 2), we next consider channel statistics that are derived from the local scattering function.

- We define the *global (or average) scattering function* of a non-WSSUS channel via the marginal

$$\overline{\mathcal{C}}_{\mathbf{H}}(\tau, \nu) \triangleq \iint \mathcal{C}_{\mathbf{H}}(t, f; \tau, \nu) dt df = \mathbb{E}\{|S_{\mathbf{H}}(\tau, \nu)|^2\}.$$

Furthermore, since $L_{\mathbf{H}}(t, f)$ can be interpreted as channel gain at time t and frequency f , we define a *TF path loss* as

$$\rho_{\mathbf{H}}^2(t, f) \triangleq \iint \mathcal{C}_{\mathbf{H}}(t, f; \tau, \nu) d\tau d\nu = \mathbb{E}\{|L_{\mathbf{H}}(t, f)|^2\}. \quad (7)$$

In the WSSUS case, $\tilde{\rho}_{\mathbf{H}}^2(t, f) = \tilde{\rho}_{\mathbf{H}}^2$. Note that the above marginal properties imply that the local scattering function is predominantly positive.

- Integrating the local scattering function with respect to f averages out the frequency dependence of the scatterer powers and thereby yields a *time-varying scattering function*,

$$\tilde{\mathcal{C}}_{\mathbf{H}}(t; \tau, \nu) \triangleq \int \mathcal{C}_{\mathbf{H}}(t, f; \tau, \nu) df.$$

- We define *TF dependent delay and Doppler profiles* as

$$\mathcal{P}_{\mathbf{H}}(t, f; \tau) \triangleq \iint \mathcal{C}_{\mathbf{H}}(t, f; \tau, \nu) d\nu \quad (8)$$

$$\mathcal{Q}_{\mathbf{H}}(t, f; \nu) \triangleq \iint \mathcal{C}_{\mathbf{H}}(t, f; \tau, \nu) d\tau. \quad (9)$$

In the case of a WSSUS channel, $\mathcal{P}_{\mathbf{H}}(t, f; \tau) = P_{\mathbf{H}}(\tau)$ and $\mathcal{Q}_{\mathbf{H}}(t, f; \nu) = Q_{\mathbf{H}}(\nu)$.

- Integrating the TF dependent delay (Doppler) profile with respect to f, τ (f, ν) defines a *time-varying path loss*

$$\tilde{\rho}_{\mathbf{H}}^2(t) \triangleq \int \mathcal{P}_{\mathbf{H}}(t, f; \tau) df d\tau = \int \mathcal{Q}_{\mathbf{H}}(t, f; \nu) df d\nu.$$

For a normalized white stationary transmit signal $s(t)$, there is $\mathbb{E}\{|r(t)|^2\} = \tilde{\rho}_{\mathbf{H}}^2(t)$.

3.2. Channel Correlation Function

Definition and Interpretation. The local scattering function describes the time- and frequency-dependent average power of scatterers with delay τ and Doppler ν . However, it does not characterize the correlation of these scatterers. To this end, we introduce a novel *channel correlation function*

$$\begin{aligned} \mathcal{A}_{\mathbf{H}}(\Delta t, \Delta f; \Delta\tau, \Delta\nu) &\triangleq \iint R_L(t, f; \Delta t, \Delta f) e^{-j2\pi(t\Delta\nu - f\Delta\tau)} dt df \\ &= \iint R_S(\tau, \nu; \Delta\tau, \Delta\nu) e^{-j2\pi(\tau\Delta f - \nu\Delta t)} d\tau d\nu. \end{aligned}$$

As required for a correlation function, $|\mathcal{A}_{\mathbf{H}}(\Delta t, \Delta f; \Delta\tau, \Delta\nu)|$ is symmetric and assumes its maximum at the origin, i.e.,

$$\begin{aligned} |\mathcal{A}_{\mathbf{H}}(\Delta t, \Delta f; \Delta\tau, \Delta\nu)| &= |\mathcal{A}_{\mathbf{H}}(-\Delta t, -\Delta f; -\Delta\tau, -\Delta\nu)| \\ &\leq \mathcal{A}_{\mathbf{H}}(0, 0; 0, 0). \end{aligned}$$

In the case of WSSUS channels, scatterers with different delays ($\Delta\tau \neq 0$) or different Doppler shifts ($\Delta\nu \neq 0$) are uncorrelated, i.e., $\mathcal{A}_{\mathbf{H}}(\Delta t, \Delta f; \Delta\tau, \Delta\nu) = R_{\mathbf{H}}(\Delta t, \Delta f) \delta(\Delta\tau) \delta(\Delta\nu)$. The interpretation of $\mathcal{A}_{\mathbf{H}}(\Delta t, \Delta f; \Delta\tau, \Delta\nu)$ as scatterer correlation is further corroborated by the relations

$$\begin{aligned}\mathcal{A}_{\mathbf{H}}(\Delta t, \Delta f; 0, 0) &= \iint R_L(t, f; \Delta t, \Delta f) dt df, \\ \mathcal{A}_{\mathbf{H}}(0, 0; \Delta\tau, \Delta\nu) &= \iint R_S(\tau, \nu; \Delta\tau, \Delta\nu) d\tau d\nu.\end{aligned}$$

The first equation shows that for $\Delta\tau = \Delta\nu = 0$, the channel correlation equals the average (over all t and f) correlation of transfer function values $L_{\mathbf{H}}(t, f + \Delta f)$ and $L_{\mathbf{H}}(t - \Delta t, f)$ separated by Δt and Δf . Similarly, for $\Delta t = \Delta f = 0$, the channel correlation equals the average (over all τ and ν) correlation of all scatterer reflectivities $S_{\mathbf{H}}(\tau, \nu + \Delta\nu)$ and $S_{\mathbf{H}}(\tau - \Delta\tau, \nu)$ separated by $\Delta\tau$ and $\Delta\nu$.

Relation to Local Scattering Function. The channel correlation function can be shown to be in 4-D Fourier relation with the local scattering function,

$$\begin{aligned}\mathcal{A}_{\mathbf{H}}(\Delta t, \Delta f; \Delta\tau, \Delta\nu) &= \iiint\!\!\!\int \mathcal{C}_{\mathbf{H}}(t, f; \tau, \nu) e^{-j2\pi(t\Delta\nu - f\Delta\tau)} \\ &\quad \times e^{-j2\pi(\tau\Delta f - \nu\Delta t)} dt df d\tau d\nu.\end{aligned}\quad (10)$$

This relation has several important aspects:

- In the WSSUS case, (10) reduces to the 2-D Fourier relation (3) connecting the scattering function $C_{\mathbf{H}}(\tau, \nu)$ and the TF correlation function $R_{\mathbf{H}}(\Delta t, \Delta f)$.
- Eq. (10) shows that $t \leftrightarrow \Delta\nu$ and $f \leftrightarrow \Delta\tau$ are (Fourier) dual variables. Thus, the variation of $\mathcal{C}_{\mathbf{H}}(t, f; \tau, \nu)$ with respect to t and f is determined by the spread of $\mathcal{A}_{\mathbf{H}}(\Delta t, \Delta f; \Delta\tau, \Delta\nu)$ in the $\Delta\nu$ and $\Delta\tau$ direction, respectively (i.e., by the amount of scatterer correlation). Denoting the maximum (effective) delay and Doppler correlation by $\Delta\tau_{\max}$ and $\Delta\nu_{\max}$, respectively, it is reasonable to define the channel's *stationarity time* T_s and *stationarity bandwidth* F_s as

$$T_s \triangleq \frac{1}{\Delta\nu_{\max}}, \quad F_s \triangleq \frac{1}{\Delta\tau_{\max}}.\quad (11)$$

Within time intervals of duration T_s and frequency bands of width F_s , $\mathcal{C}_{\mathbf{H}}(t, f; \tau, \nu)$ is (effectively) constant as a function of t and f (for τ, ν fixed). For WSSUS channels, the scatterers are uncorrelated and thus $\Delta\tau_{\max} = \Delta\nu_{\max} = 0$ and $T_s = F_s = \infty$. This agrees with the fact that here $\mathcal{C}_{\mathbf{H}}(t, f; \tau, \nu) = C_{\mathbf{H}}(\tau, \nu)$ is independent of t and f .

- Similarly, according to (10) $\tau \leftrightarrow \Delta f$ and $\nu \leftrightarrow \Delta t$ are (Fourier) dual. Hence, the decay of $\mathcal{A}_{\mathbf{H}}(\Delta t, \Delta f; \Delta\tau, \Delta\nu)$ with respect to Δt and Δf is determined by the extension of $\mathcal{C}_{\mathbf{H}}(t, f; \tau, \nu)$ in the ν and τ direction, respectively, i.e., by the amount of Doppler and delay. Denoting the maximum effective delay and maximum effective Doppler frequency by τ_{\max} and ν_{\max} , respectively, it makes sense to define the channel's *coherence time* and *coherence bandwidth* as³

$$T_c \triangleq \frac{1}{\nu_{\max}}, \quad F_c \triangleq \frac{1}{\tau_{\max}}.\quad (12)$$

³Note that there exist formally different but conceptually similar definitions of coherence time and coherence bandwidth [4, 5].

4. DOUBLY UNDERSPREAD CHANNELS

Definition. We call a non-WSSUS channel (*dispersion underspread*) if its time/frequency (delay/Doppler) dispersiveness in a certain sense is “small,” i.e., if for arbitrary t, f the local scattering function $\mathcal{C}_{\mathbf{H}}(t, f; \tau, \nu)$ is effectively nonzero only for (τ, ν) close to $(0, 0)$. More formally, we require that

$$d_{\mathbf{H}} \triangleq \tau_{\max} \nu_{\max} \leq 1,\quad (13)$$

with τ_{\max} (ν_{\max}) being the channel's maximum effective delay (Doppler frequency) and $d_{\mathbf{H}}$ denoting the channel's delay/Doppler (dispersion) spread. Eq. (13) naturally extends the dispersion underspread property of WSSUS channels (cf. [1, 3]). If (13) is satisfied, (12) implies $T_c F_c \geq 1$, i.e., that the channel transfer function $L_{\mathbf{H}}(t, f)$ varies only slowly.

We next complement the dispersion underspread property by a *correlation underspread* property that is important for $\mathcal{C}_{\mathbf{H}}(t, f; \tau, \nu)$ to be physically meaningful. Motivated by the interpretation of $\mathcal{A}_{\mathbf{H}}(\Delta t, \Delta f; \Delta\tau, \Delta\nu)$ as scatterer correlation, we define a channel to be correlation underspread if $\mathcal{A}_{\mathbf{H}}(\Delta t, \Delta f; \Delta\tau, \Delta\nu)$ is concentrated about the origin, i.e., if

$$c_{\mathbf{H}} \triangleq T_c F_c \Delta\tau_{\max} \Delta\nu_{\max} \leq 1,\quad (14)$$

with $c_{\mathbf{H}}$ denoting the channel's correlation spread and $T_c, F_c, \Delta\tau_{\max}, \Delta\nu_{\max}$ being the coherence time, coherence bandwidth, maximum (effective) delay correlation, and maximum (effective) Doppler correlation, respectively, of the channel.

By combining the dispersion and correlation underspread properties, we call a non-WSSUS channel *doubly underspread* if (13) and (14) are satisfied simultaneously. Using the relations (11) and (12), these conditions can alternatively be expressed by the two equivalent double inequalities

$$\Delta\tau_{\max} \Delta\nu_{\max} \leq \tau_{\max} \nu_{\max} \leq 1, \quad \text{or} \quad T_s F_s \geq T_c F_c \geq 1.$$

The first double inequality requires that i) the channel is dispersion underspread and ii) only delay/Doppler components close to each other are correlated. The second inequality means that i) the channel (transfer function) varies only slowly and ii) the variation of the channel statistics is even slower than that of the channel (transfer function).

Example and Physical Interpretation. We illustrate the concept of doubly underspread channels by a simple example; this example also serves to establish relations to geometric properties of the physical propagation environment. We consider a typical cellular mobile radio system operating at $f_c = 2$ GHz in a suburban environment. The mobile's maximum speed is assumed to be $v_0 = 15$ m/s which corresponds to a maximum Doppler frequency of $\nu_{\max} = \frac{v_0}{c} f_c = 100$ Hz. With the maximum path length between base station and mobile assumed to be $d = 3$ km, it follows that delays up to $\tau_{\max} = \frac{d}{c} = 10 \mu\text{s}$ can occur. With (12) we thus obtain $T_c = 10$ ms and $F_c = 100$ kHz. With (13), we obtain $d_{\mathbf{H}} = 10^{-3} \ll 1$, i.e., a dispersion underspread channel.

Typically, the main mechanism causing scatterers (reflectivities) to be correlated is that they correspond to the same physical object (building surface etc.). Assuming the maximum spatial extension and angular spread of the scatterers to be $w = 30$ m and $\delta = 3^\circ$ implies $\Delta\tau_{\max} = \frac{w}{c} = 0.1 \mu\text{s}$ and $\Delta\nu_{\max} = \nu_{\max} \sin(\delta) \approx 5.2$ Hz. With (11), we then obtain $T_s = 191$ ms and $F_s = 10$ MHz. Furthermore, (14) yields $c_{\mathbf{H}} = 5.2 \cdot 10^{-4} \ll 1$ and thus a correlation underspread channel. We conclude that the channels in this environment are doubly underspread.

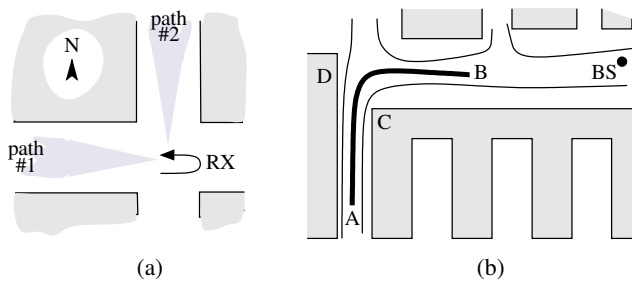


Figure 1: Propagation environments for (a) simulated and (b) measured channel (dark gray indicates buildings).

Implications. The double underspread property has important consequences for the interpretation and use of the local scattering function (full details are presented in [13]):

- The local scattering function of doubly underspread channels is effectively real-valued and positive. In contrast, for non-WSSUS channels that are not doubly underspread we obtain significant imaginary/negative components.
- For doubly underspread channels, $\mathcal{C}_{\mathbf{H}}(t, f; \tau, \nu)$ is a smooth function of t and f , i.e., scatterer properties (power, delay, Doppler) change only slowly over time and frequency.
- Within time intervals of duration T_s and frequency bands of width F_s , doubly underspread channels can locally be approximated by (properly chosen) WSSUS channels (this is similar to Bello’s quasi-WSSUS channels [2]).
- Doubly underspread channels allow to separate the randomness and the TF-variations of the channel via a 2-D Karhunen-Loève expansion involving a simple TF localization filter, TF shifts, and uncorrelated random weights.

5. NUMERICAL RESULTS

Simulated Channel. We first consider a synthetical example for a mobile radio system with carrier frequency 2GHz. The (non-line-of-sight) urban propagation scenario is shown in Fig. 1(a). The base station is assumed to be located somewhere in the north-west. The mobile (labeled ‘RX’) is assumed to perform a U-turn at the crossroads with a constant speed of 2 m/s (this corresponds to a maximum Doppler frequency of $\nu_{\max} = 13.3$ Hz and a coherence time of $T_c = 75$ ms). There are two main propagation paths corresponding to two street canyons. We assume that the delay of both paths equals τ_0 , i.e., we have a flat fading channel. For each path there exist L subpaths corresponding to total angular spreads of $\delta = 5^\circ$. This non-WSSUS channel was simulated according to $h(t, \tau) = h(t) \delta(\tau - \tau_0)$ with

$$h(t) = \sum_{k=1}^2 \sum_{l=1}^L a_{k,l} e^{j\psi_{k,l}} \exp[j2\pi \nu_{\max} \cos(\phi_{k,l}(t))].$$

Here, $a_{k,l}$ and $\psi_{k,l}$ denote the random amplitude and phase of the l th subpath of the k th path. Furthermore, $\phi_{k,l}(t)$ is the incidence angle (i.e., the angle between the directions of path propagation and mobile motion) of the l th subpath of the k th path. This incidence angle was simulated by adding a (time-independent) random angular “jitter” $\Delta\phi_{k,l} \in [-\frac{\delta}{2}, \frac{\delta}{2}]$ to the time-dependent mean incidence angle $\bar{\phi}_k(t)$ associated to path $\#k$. For fixed propagation paths, the angles $\bar{\phi}_1(t)$ and $\bar{\phi}_2(t)$ are determined by the motion of the mobile.

Fig. 2(a) shows the magnitude (in dB) of a typical realization of $h(t)$. The channel’s local scattering function

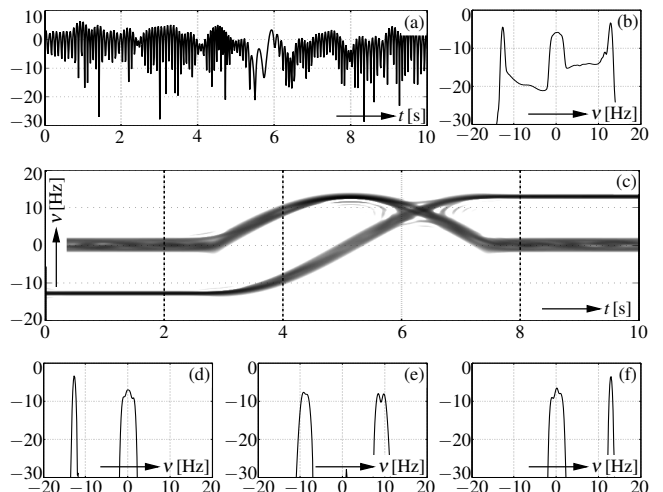


Figure 2: Simulated channel: (a) realization of $h(t)$ (magnitude in dB); (b) global scattering function for $\tau = \tau_0$; (c) local scattering function $\mathcal{C}_{\mathbf{H}}(t, f; \tau_0, \nu)$ for arbitrary f (grayscale plot, darker shading corresponds to larger values); (d)–(f) cuts of $\mathcal{C}_{\mathbf{H}}(t, f; \tau_0, \nu)$ (in dB) at arbitrary f and (d) $t = 2$ s, (e) $t = 4$ s, (f) $t = 8$ s.

$\mathcal{C}_{\mathbf{H}}(t, f; \tau_0, \nu)$ (which is independent of f and obtained by averaging over 50 channel realizations) is shown in Fig. 2(c). It clearly displays the different time intervals where the mobile moves east (0–3 s), performs the U-turn (3–7 s), and moves back west (7–10 s). In the initial phase, path #1 and #2 experience Doppler shifts of -13 Hz and 0 Hz, respectively (cf. Fig. 2(d)). During the U-turn, the Doppler frequencies gradually change from -13 Hz to 13 Hz (path #1) and from 0 Hz to 13 Hz and back to 0 Hz (path #2), cf. Fig. 2(c),(e). Finally, after the U-turn, path #1 and #2 experience Doppler shifts of 13 Hz and 0 Hz, respectively. Note that these insights cannot be gained from the global scattering function (averaged over 10 s and 50 realizations) depicted in Fig. 2(b). We finally note that the maximum Doppler correlation was estimated as $\Delta\nu_{\max} = 1.28$ Hz which corresponds to a stationarity time $T_s = 781$ ms.

Measured Channel. We next analyze measurements⁴ of a non-WSSUS channel performed in the course of the METAMORP project [14]. The propagation scenario (suburban, partial line of sight) is shown in Fig. 1(b) with the base station labeled ‘BS’. The carrier frequency was $f_c = 1792$ MHz. During the measurement period of 50.33 s, the mobile moved from position ‘A’ to position ‘B’ along the thick line with a constant velocity of 1.6 m/s (corresponding to a maximum Doppler frequency $\nu_{\max} = 9.56$ Hz). Within this period, 1024 impulse response snapshots $h(kT, \tau)$ were recorded (time increment $T = 49.152$ ms, measurement bandwidth 10 MHz).

After subtracting a (rather weak) channel mean from the measurements, an estimate of the local scattering function $\mathcal{C}_{\mathbf{H}}(t, f_c; \tau, \nu)$ was obtained using a nonstationary 2-D multiwindow estimator (note that we used only a single channel realization; for further details see [13]). Estimates of the TF dependent delay profile $\mathcal{P}_{\mathbf{H}}(t, f_c; \tau)$, the TF dependent Doppler profile $\mathcal{Q}_{\mathbf{H}}(t, f_c; \nu)$, and the TF path loss $\rho_{\mathbf{H}}^2(t, f_c)$, were computed according to (8), (9), and (7).

⁴Courtesy of T-NOVA Deutsche Telekom Innovationsgesellschaft mbH (Technologiezentrum Darmstadt, Germany). We are grateful to I. Gaspard and M. Steinbauer for providing us with the measurement data.

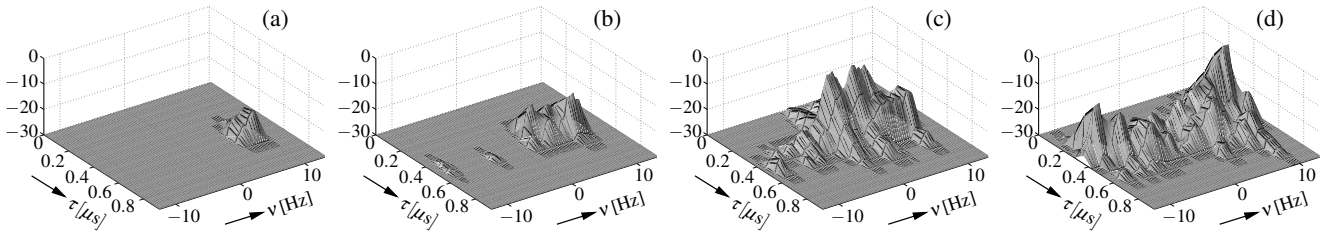


Figure 3: Four sections of the estimated local scattering function $\mathcal{C}_{\mathbf{H}}(t, f; \tau, \nu)$ (in dB) of the measured channel with $f = f_c$ fixed and (a) $t = 5$ s, (b) $t = 20$ s, (c) $t = 28$ s, (d) $t = 40$ s.

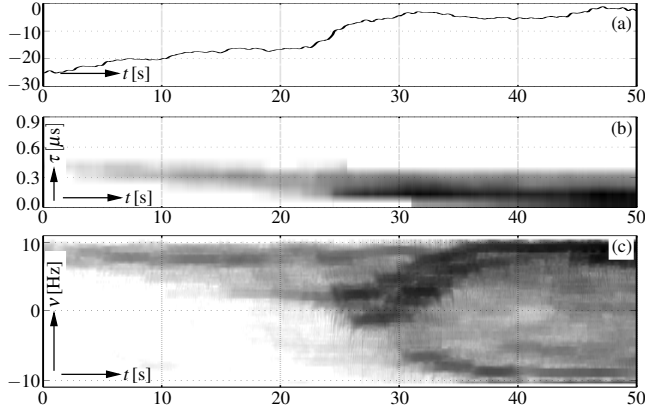


Figure 4: Results for the measured channel: (a) estimated time-varying path loss $\rho_{\mathbf{H}}^2(t, f_c)$ (in dB); (b) estimated time-varying delay profile $\mathcal{P}_{\mathbf{H}}(t, f_c; \tau)$; (c) estimated time-varying Doppler profile $\mathcal{Q}_{\mathbf{H}}(t, f_c; \nu)$.

The results are shown in Figs. 3 and 4 and can be interpreted as follows. During the first 25 s, there is no line of sight and thus shadowing causes a large path loss (cf. Figs. 3(a),(b) and 4(a)). Furthermore, the Doppler frequencies close to ν_{\max} indicate that the angle of arrival (AOA) of all paths is about 0° , i.e., the dominant waves arrive through the street from ahead of the mobile (cf. Figs. 3(a),(b) and 4(c)). As the mobile approaches the corner (labeled ‘C’ in Fig. 1(b)), the delays gradually drift from $\tau_{\max} = 0.5$ to $0.3 \mu\text{s}$ (see Figs. 3(b) and 4(b)) and the spread of the Doppler components grows since the scatterer’s angular spread and thus the AOA spread increases (cf. Figs. 3(b) and 4(c)). After 25 s, the mobile passes the corner. This results in a line-of-sight component and a significantly smaller path loss. The dominant components arrive from broadside (AOA 90° and Doppler frequency ≈ 0 Hz) as can be seen in Figs. 3(c) and 4(c). After the mobile turned right, the dominant components arrive from ahead (AOA $\approx 0^\circ$, Doppler frequency $\approx \nu_{\max}$); furthermore, delays drift from 0.3 to $0.1 \mu\text{s}$ (see Figs. 4(c) and 3(c)). During the last 20 seconds, a second contribution with Doppler frequency $\approx -\nu_{\max}$ is seen in Fig. 4(c); however, only the local scattering function in Fig. 3(d) shows the larger delay of this component and allows to associate it to a building (labeled ‘D’ in Fig. 1(b)).

Finally, we determined the estimates $T_c = 105$ ms, $F_c = 2$ MHz, $\Delta\tau_{\max} \leq 0.1 \mu\text{s}$, and $\Delta\nu_{\max} = 0.38$ Hz. This corresponds to a stationarity time $T_s = 2.6$ s and a stationarity bandwidth $F_s \geq 10$ MHz. (The measurement bandwidth of 10 MHz was too small to determine $\Delta\tau_{\max}$ and F_s more exactly.) With these parameters, we obtain a dispersion spread $d_{\mathbf{H}} = 4.8 \cdot 10^{-6}$ and a correlation spread $c_{\mathbf{H}} = 8 \cdot 10^{-3}$. Hence, this channel is seen to be doubly underspread.

6. CONCLUSIONS

We introduced novel tools for the statistical characterization of non-WSSUS fading dispersive channels and demonstrated their relevance for practical wireless propagation scenarios. Further results regarding doubly underspread channels and the estimation of non-WSSUS channel statistics are presented in [13]. We expect that our theoretical framework is useful for realistic channel simulation, performance analysis of wireless communication schemes, and improved transmitter/receiver design. Finally, the stationarity time and bandwidth are relevant for assessing transmission methods exploiting long-term channel properties.

REFERENCES

- [1] J. G. Proakis, *Digital Communications*. New York: McGraw-Hill, 3rd ed., 1995.
- [2] P. A. Bello, “Characterization of randomly time-variant linear channels,” *IEEE Trans. Comm. Syst.*, vol. 11, pp. 360–393, 1963.
- [3] R. S. Kennedy, *Fading Dispersive Communication Channels*. New York: Wiley, 1969.
- [4] T. S. Rappaport, *Wireless Communications: Principles & Practice*. Upper Saddle River (NJ): Prentice Hall, 1996.
- [5] J. D. Parsons, *The Mobile Radio Propagation Channel*. London: Pentech Press, 1992.
- [6] A. Gehring, M. Steinbauer, I. Gaspard, and M. Grigat, “Empirical channel stationarity in urban environments,” in *Proc. EPMCC 2001*, (Vienna, Austria), Feb. 2001.
- [7] R. J. C. Bultitude, G. Brussaard, M. H. A. J. Herben, and T. J. Willink, “Radio channel modelling for terrestrial vehicular mobile applications,” in *Proc. Millenium Conf. Antennas and Propagation*, (Davos, Switzerland), April 2000.
- [8] B. H. Fleury and P. E. Leuthold, “Radiowave propagation in mobile communications: An overview of European research,” *IEEE Comm. Mag.*, vol. 34, pp. 70–81, Feb. 1996.
- [9] R. Heddergott, U. P. Bernhard, and B. H. Fleury, “Stochastic radio channel model for advanced indoor mobile communication systems,” in *Proc. PIMRC-97*, (Helsinki, Finland), pp. 140–144, Sept. 1997.
- [10] L. M. Correia, ed., *Wireless Flexible Personalised Communications (COST 259 Final Report)*. Chichester (UK): Wiley, 2001.
- [11] L. A. Zadeh, “Frequency analysis of variable networks,” *Proc. of IRE*, vol. 76, pp. 291–299, March 1950.
- [12] P. Flandrin, *Time-Frequency/Time-Scale Analysis*. San Diego (CA): Academic Press, 1999.
- [13] G. Matz, “Doubly underspread non-WSSUS channels: Analysis and estimation of channel statistics,” in *Proc. IEEE SPAWC-03*, (Rome, Italy), June 2003.
- [14] <http://www.nt.tuwien.ac.at/mobile/projects/METAMORP>.